

Effects of Metallicity on the Rotational Velocities of Massive Stars

Laura R. Penny, Amanda J. Sprague, George Seago

Department of Physics and Astronomy

The College of Charleston

Charleston, SC 29424

pennyl@cofc.edu, ajspragu@edisto.cofc.edu, gseago@edisto.cofc.edu

Douglas R. Gies

Center for High Angular Resolution Astronomy and

Department of Physics and Astronomy,

Georgia State University, Atlanta, GA 30303-3083

gies@chara.gsu.edu

ABSTRACT

Recent theoretical predictions for low metallicity massive stars predict that these stars should have drastically reduced equatorial winds (mass loss) while on the main sequence, and as such should retain most of their angular momentum. Observations of both the Be/(B+Be) ratio and the blue-to-red supergiant ratio appear to have a metallicity dependence that may be caused by high rotational velocities. We have analyzed 39 archival *Hubble Space Telescope Imaging Spectrograph (STIS)*, high resolution, ultraviolet spectra of O-type stars in the Magellanic Clouds to determine their projected rotational velocities $V \sin i$. Our methodology is based on a previous study of the projected rotational velocities of Galactic O-type stars using *International Ultraviolet Explorer (IUE)* Short Wavelength Prime (SWP) Camera high dispersion spectra, which resulted in a catalog of $V \sin i$ values for 177 O stars. Here we present complementary $V \sin i$ values for 21 Large Magellanic Cloud and 22 Small Magellanic Cloud O-type stars based on STIS and IUE UV spectroscopy. The distribution of $V \sin i$ values for O type stars in the Magellanic Clouds is compared to that of Galactic O type stars. Despite the theoretical predictions and indirect observational evidence for high rotation, the O type stars in the Magellanic Clouds do not appear to rotate faster than their Galactic counterparts.

Subject headings: Stars: spectroscopic — stars: early-type — stars: rotation — Magellanic Clouds — ultraviolet: stars

1. Introduction

What effect does metallicity have on the mass loss and angular momentum loss of massive stars? There is a large amount of secondary evidence, some of which is summarized below, suggesting that low metallicity should result in smaller angular momentum loss and subsequently higher rotational velocities for these type stars. However, there is an unfortunate lack of direct measurements of the equatorial rotational velocity V_{rot} , or even of the projected rotational velocity $V \sin i$ for massive stars in a low Z environment. The Large and Small Magellanic Clouds (LMC & SMC) are nearby, contain many young massive objects, and have low Z values of 0.007 and 0.004, respectively. As such they present an ideal laboratory to test the dependence of massive star rotation on metallicity.

Maeder, Grebel, & Mermilliod (1999) found a significant increase in the number ratio of Be/(B+Be) stars with decreasing metallicity among Galactic and MC clusters (see, however, the counterarguments presented by Keller et al. 1999). The Be phenomenon is closely linked to rapid rotation (Porter & Rivinius 2003). To explain this trend in Be star number ratio, the authors raise the possibility that stars forming in a low metallicity environment would have higher initial rotational velocities. Although no numerical models of the formation of massive stars at low Z have been produced, the authors tentatively present some possible origins of these higher initial rotational velocities. A lower Z environment would have lower dust content and fewer metallic ions present in star forming regions so that the magnetic field of the contracting central mass is less coupled to the surrounding region. Also the lifetime of the accretion disk is likely related to its opacity, which will decrease with lower metallicity. These factors would result in less angular momentum loss during star formation, leading to higher initial rotational velocities. The possibility of faster initial rotation at low metallicity resulting in more rotational mixing on the main sequence has also been suggested to resolve the nitrogen enrichment seen in SMC B- and A-supergiants (Venn et al. 1998). Maeder et al. (1999) state “Of course, direct observations of $V \sin i$ in LMC and SMC clusters are very much needed in order to substantiate the above results.”

Observations of the number ratio of blue to red supergiants in nearby galaxies also show a sharp dependence upon metallicity (Humphreys & McElroy 1984). Stellar interior models which include rotation can account for this long-standing problem (Maeder & Meynet 2001). The primary cause of this is the mild mixing just outside the core of a rotating star during the main sequence. This increases the amount of helium near and above the H-shell. The net effect of the larger He core and the mild main sequence mixing is to decrease the importance of the convective zone above the H-burning shell in the post-main sequence evolution. Because of the small polytropic index in the convective zone, the larger the size of the zone the smaller the radius of the star. Conversely, if its contribution is small, the

overall size of the star increases, leading to a redward position in the Hertzsprung-Russell (HR) diagram.

Another key prediction of these new models is shown by comparing Figure 10 of Meynet & Maeder (2000) and Figure 3 of Maeder & Meynet (2001). These are plots of the evolution of surface rotational velocities for massive stars in both Galactic and SMC metallicity, respectively. At low Z , the surface rotational velocities will remain almost constant during the main sequence evolution, contrary to that of massive stars at solar metallicity where the rotational velocities are predicted to rapidly decrease. Theoretically this results from both lower equatorial mass loss and the outward transport of angular momentum from the interior of the star by meridional circulation. Models of massive stars at both metallicities show a drastic decrease in rotational velocity after the terminal age main sequence.

The idea that a low metallicity environment would create massive, rapidly rotating, helium stars has even been raised by theorists as a possible source of gamma-ray burst progenitors (MacFadyen & Woosley 1999). Here the outer layers of the star, and, in at least some cases, the mantle have too much angular momentum to fall freely inside the last stable orbit during core collapse. An accretion disk forms where the dissipation of rotational and gravitational energy will give rise to some sort of mass ejection and electromagnetic radiation, a “hypernova.” This results in the prompt formation of a black hole through hyperaccretion.

2. Projected Rotational Velocities from UV lines

Stellar rotation is the dominant process in shaping the photospheric lines of O stars. The vast number of lines present in the ultraviolet spectra of O-type stars suggests that accurate projected rotational velocities could be found by studying these objects in the ultraviolet. These lines arise from high excitation transitions from deeper in the photosphere, and they are less subject to wind variability than optical lines. Also they are less likely to be contaminated by weak emission from circumstellar and nebular gas. The standard method of individual profile fitting in the UV is difficult because of line blending. A powerful alternative involves cross-correlation of a narrow-lined star with a test star, which will result in a cross-correlation function (ccf) that represents a “superline” of the test star. This technique actually increases the S/N of the observed spectrum by in effect combining all the UV lines into one. The “superline” will have an observed width related to the line width of the test star and that of the narrow-lined star (Figure 1). Fitting this “superline” is the numerical equivalent of fitting each UV absorption feature and combining the resulting measurements. Our previously derived $V \sin i$ values for 177 Galactic O stars were calculated by calibrating

the widths of cdfs derived from *IUE* SWP high dispersion spectra as a function of published $V \sin i$ values from Conti & Ebbets (1977) in a common sample of objects (Penny 1996 = P96). Conti & Ebbets (1977) fit artificially broadened model line profiles (from the non-LTE model atmospheres of Auer & Mihalas 1972) of four visual absorption lines to determine their $V \sin i$ values. The lines used were $H\gamma$ $\lambda 4340$, He I $\lambda 4388$ and $\lambda 4471$, and He II $\lambda 4541$. Howarth et al. (1997) performed a cross-correlation study similar to ours with *IUE* high resolution spectra of 373 OB-type stars using the template star τ Sco = HD 149438 (B0.2 IV). Although their calibration technique differed slightly from ours, their findings supported those from our study.

3. Observations and Reductions

Methods similar to those above can be utilized with observations of O-type stars made with the Space Telescope Imaging Spectrograph (STIS) E140M grating. The E140M grating produces in a single exposure an echelle spectrogram covering the wavelength interval 1150 – 1700Å, with an effective spectral resolving power of $R = 46,000$. This grating set up is complementary to the *IUE* SWP arrangement which was used so effectively to obtain an almost complete catalog of UV observations of Galactic O-type stars to $V \approx 11$. The Multimission Archive at Space Telescope (MAST¹) contains spectra of the 18 SMC and 6 LMC O-type stars observed with this grating. There are also STIS E140M grating archival spectra of 12 Galactic O-type stars which we obtained in order to calibrate our methodology with the STIS observations. Although the E140M spectra are similar in many ways to the SWP high resolution spectra in our previous methodology, it is prudent to use these overlapping Galactic stars as an experimental checks of our calibration. There are also available in MAST *IUE* SWP high resolution spectra of 4 SMC and 16 LMC O-type stars; one of the latter is among those with archival STIS spectra.

The NEWSIPS MXHI files of the above SWP spectra are spectrograms that cover the wavelength region of 1200 – 1900Å. The archival STIS spectra are in extracted one dimensional FITS format, forming a near complete spectrogram covering the wavelength range 1150 – 1700Å. We use a series of routines we have written in the Interactive Data Language² to further reduce the spectra (see details in Penny, Gies, & Bagnuolo 1997). One of the most important steps in our reduction is the placement of the data on a $\log \lambda$ grid, in which each pixel step corresponds to a uniform velocity step of 1 pixel = 10 km s⁻¹. The

¹URL: <http://archive.stsci.edu/>

²IDL is a registered trademark of Research Systems, Inc.

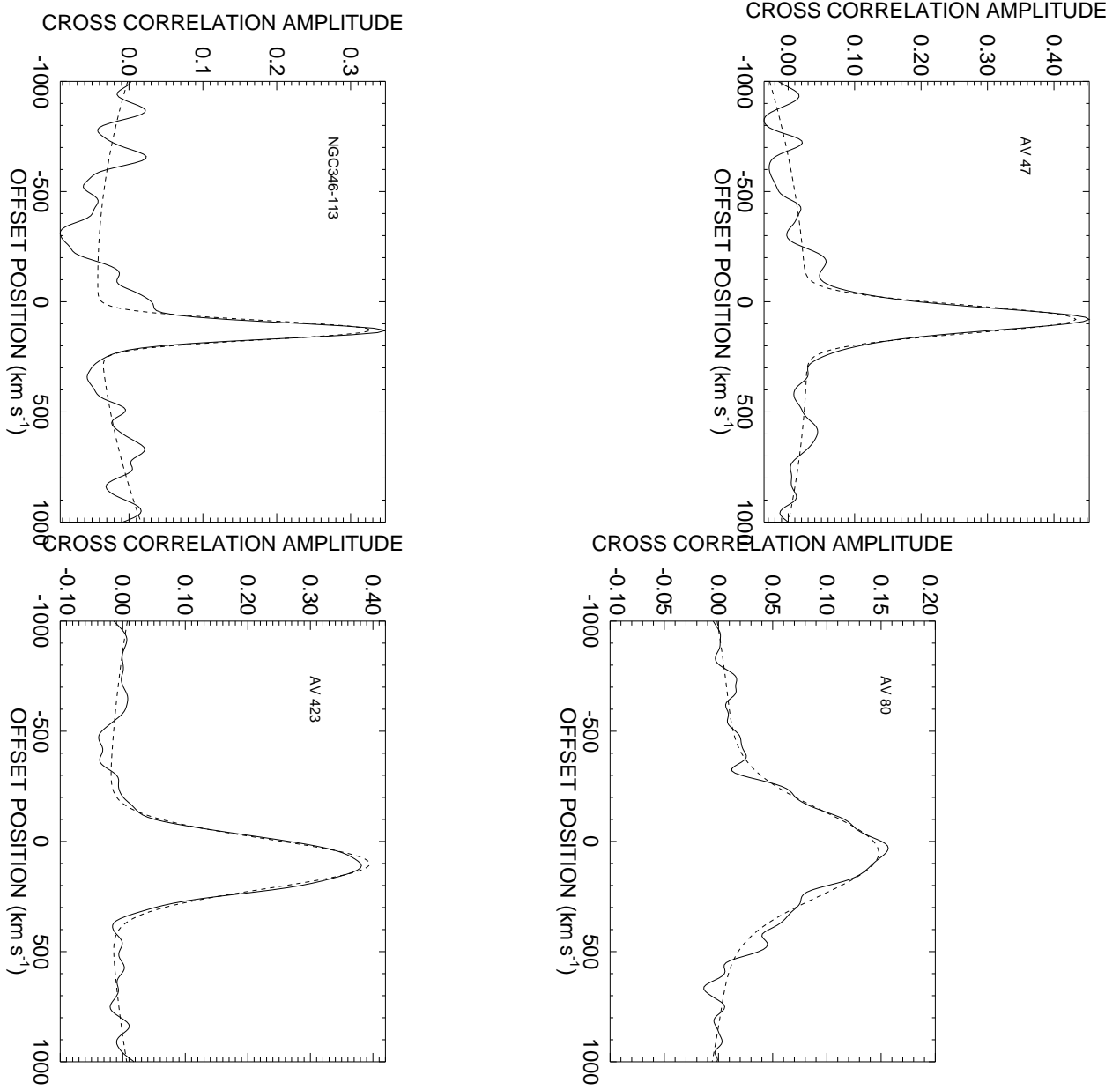


Fig. 1.— The cross-correlation functions and Gaussian fits for the SMC stars (a) NGC346-113 (OC6 V; $V \sin i < 40 \text{ km s}^{-1}$), (b) AV 47 (O8 III(f)); $V \sin i = 76 \text{ km s}^{-1}$), (c) AV 423 (O9.5 V; $V \sin i = 186 \text{ km s}^{-1}$), (d) AV 80 (O4-6n(f)p; $V \sin i = 324 \text{ km s}^{-1}$). The bumpy nature of the ccf for AV 80 may be indicative of non-radial pulsations.

spectra were smoothed using a Gaussian transfer function (FWHM = 40 km s⁻¹) and the interstellar features are removed. The spectra are then rectified to a unit continuum.

Complete lists of spectra obtained, targets, and their spectral classifications are presented in Tables 1, 2, & 3 for Galactic, SMC, and LMC targets, respectively. Spectral classifications given with square brackets are from investigators other than Walborn (see Maíz-Apellániz et al. 2004) and are taken from the compilations of Howarth & Prinja (1989), Conti & Ebbets (1977), Garmany, Conti, & Massey (1987), Conti, Garmany, & Massey (1986), Parker et al. (1992), Garmany, Massey, & Parker (1994), Massey et al. (1989), Massey, Parker, & Garmany (1989), and Massey et al. (1995). We make special note of the SMC star AV 423. This star is classified as O9.5 V by Massey et al. (1995). However, its UV spectrum, plotted in Figure 2, is inconsistent with that designation. Both Si IV $\lambda\lambda$ 1400 and C IV $\lambda\lambda$ 1550 doublets have P Cygni profiles, which makes this only the third star known in the SMC with Si IV emission. This feature in SMC is indicative of a supergiant classification. However, the N V doublet is extremely weak even in absorption. In addition to AV 423, we also plot AV 15 [O6.5 II(f)], AV 83 [O7 Iaf+], and NGC346-12 [O9.5-B0 V] for comparison in Figure 2. Whatever the revised type of AV 423, it is clearly not a dwarf star, and we will treat it as an evolved object below.

4. Projected Rotational Velocities from Cross-Correlation Functions

The spectra for each star are cross-correlated with a narrow-lined template star. We actually cross-correlate each test star with four different templates in order to get the best (usually highest) peak for fitting. These templates are HD 34078 (O9.5 V; $V \sin i = 25$ km s⁻¹), HD 149438 (B0.2 IV; $V \sin i < 5$ km s⁻¹), HD 54662 (O6.5 V; $V \sin i = 85$ km s⁻¹), and HD 57682 (O9 IV; $V \sin i = 33$ km s⁻¹). We cross-correlate essentially the full wavelength range of the spectra (STIS: 1200 – 1700Å; IUE: 1200 – 1900Å), setting to unity regions surrounding the strong P Cygni lines of N V λ 1240, Si IV λ 1400, and C IV λ 1550, since these features reflect wind and not photospheric rotational motion. The region around Ly α is also set to unity. The spectra are padded with 1000 km s⁻¹ of artificial continuum on both ends to include the entire observed range in the cross-correlation. The cross-correlation function (ccf) is the sum of the square of the differences between the test spectrum and the reference spectrum shifted in velocity from –1000 km s⁻¹ to +1000 km s⁻¹ at 10 km s⁻¹ intervals. The ccfs are rectified and inverted for convenience in fitting and plotting. Each ccf is then fitted with a Gaussian function, and $V \sin i$ values are derived from the Gaussian widths using the calibrations presented in P96 (HD 34078), Penny et al. (2001, HD 149438), Penny et al. (1997, HD 54662), and Penny (1997, HD 57682). We adopt 40 km s⁻¹ as our

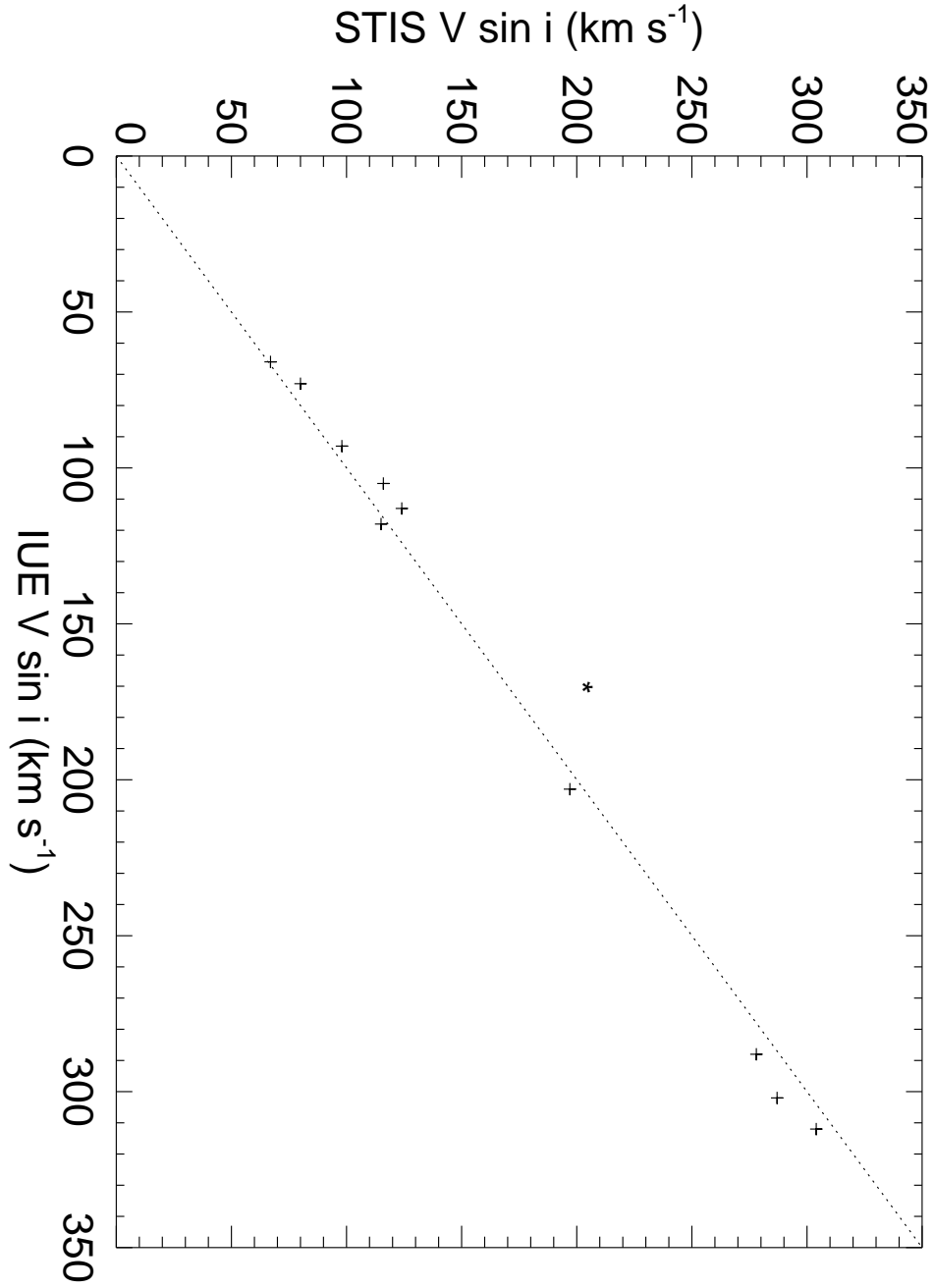


Fig. 2.— Projected rotational velocities from STIS spectra versus those from *IUE* spectra for 12 Galactic O-type stars. The asterisk is plotted for the values for HD 13745, which may display time variations in line width (see §4).

minimum measurable $V \sin i$, as this is the FWHM of the Gaussian transfer function used to smooth the data.

We compared $V \sin i$ values from our previous study to those obtained using STIS observations for those Galactic O-type stars in common. This is especially important since the wavelength range in the STIS spectra is smaller than that of the *IUE* observations, which might introduce systematic differences in our $V \sin i$ values. We plot in Figure 3 $V \sin i$ values from the STIS observations versus those from the *IUE* observations. We see excellent agreement, well within our estimated errors from the *IUE* data ($\pm 2 - 5\%$), with the exception of HD 13745. This star is noted in P96 as being a possible unresolved double-lined spectroscopic binary or it may be a short period pulsator (Koen & Eyer 2002), so a larger than expected difference in $V \sin i$ here is not unexpected.

Our calculated projected rotational velocities are presented in Tables 2 and 3. Previous estimates of $V \sin i$ for the SMC stars in common by Walborn et al. (2000) are also shown in Table 2. We note that they describe their values as preliminary due to the blended nature of the He I + He II $\lambda 4026$ line from which their estimates are determined. Nevertheless, there is reasonable agreement between our results except in the cases of NGC346-324 and AV 47, which may be spectroscopic binaries observed at differing orbital phases. The SMC contains both the slowest and fastest rotators among our sample of Magellanic Cloud stars. Both NGC346-113 and AV 220 have narrow-lined spectra indicating a $V \sin i$ below the minimum for which we can determine an accurate projected rotational velocity ($< 40 \text{ km s}^{-1}$). The fastest rotator is AV 80 that has a $V \sin i$ comparable to that found in some Be stars. Walborn et al. (2000) show that the He II $\lambda 4686$ feature is a double-peaked emission line in this star, which suggests that this star may have a disk-like circumstellar envelope, again like those found in Be stars.

5. Results and Conclusions

While our ultimate goal is to determine the true rotational velocities of O-type stars in differing environments, in general only the projected rotational velocities are measurable. However, we can make some statistical arguments. The inclination angles of the polar axes i of a group of stars should be randomly distributed. For each metallicity environment (Galactic, LMC, and SMC) we expect that the distribution of i should be the same, that is random. Thus, we can safely intercompare the rotational properties through an examination of their projected rotational velocities. We can compare the projected rotational velocity distributions of the different groups of star by calculating their cumulative distribution function (cdf), as shown in Howarth et al. (1997) and Howarth & Smith (2001). The cdf gives

Table 1. Galactic Targets

Star	Spectral Classification	$\langle V \sin i \rangle$ (this paper) (km s ⁻¹)	$\langle V \sin i \rangle$ (P96) (km s ⁻¹)	SWP #	STIS data set
HD 14434	O5.5 Vn((f))p	377	368	16094	O63508010
HD 63005	[O6 V]	80	73	21506	O63531010
HD 13268	[O7]	287	302	9323	O63506010
HD 152590	O7.5 V	67	66	16098	O6LZ67010
HD 12323	ON9 V	124	113	9652	O63505010
HD 91651	O9 V:n	278	288	14830	O6LZ34010
HD 156359	[O9 III]	98	93	11274	O6LZ70010
HD 210809	O9 Iab	115	118	9103	O6359T010
HD 308813	O9.5 V	197	203	21172	O63559010
HD 168941	O9.5 II-III	116	105	23843	O6LZ81010
HD 92554	[O9.5 II]	304	312	16220	O6LZ36010
HD 13745	O9.7 II((n))	196	168	16111	O6LZ05010

Table 2. Small Magellanic Cloud Targets

Star	Spectral Classification	$\langle V \sin i \rangle$ (this paper) (km s ⁻¹)	$\langle V \sin i \rangle$ (W00) (km s ⁻¹)	SWP # or STIS data set
NGC346-355	O2 III(f*)	112	120	O4WR01010
AV 388	[O4 V]	179	...	SWP33968
NGC346-324	O4 V((f))	70	120	O4WR01020
NGC346-368	O4-5 V((f))	55	80	O4WR01030
AV 80	O4-6n(f)p	324	270	O4WR12010,12020
AV 75	O5 III(f+)	109	110	O4WR11010,11020
NGC346-113	OC6 Vz	< 40	45	O4WR02010
AV 243	[O6 III]	62	...	SWP33961
NGC346-487	[O6.5 V]	65	...	O4WR23010
AV 15	O6.5 II(f)	128	132	O4WR14010,14020
AV 220	O6.5f?p	< 40	62	O4WR20010,20020
SK80	[O6.5 If]	106	...	SWP06564,25438
AV 95	O7 III((f))	82	89	O4WR17010,17020
AV 26	[O7 III]	127	...	SWP32466
AV 83	O7 Iaf+	82	80	O4WR15010,15020
AV 69	OC7.5 III((f))	100	104	O4WR13010,13020
NGC346-682	[O8 V]	71	...	O4WR24010
AV 47	O8 III((f))	76	169	O4WR16010,16020
AV 423	[O9.5 V](?)	186	...	O4WR18010,18020
NGC346-12	O9.5-B0 V	67	84	O4WR21010
AV 327	O9.5 II-Ibw	71	80	O4WR30010,30020
AV 170	O9.7 III	54	65	O4WR18010,18020

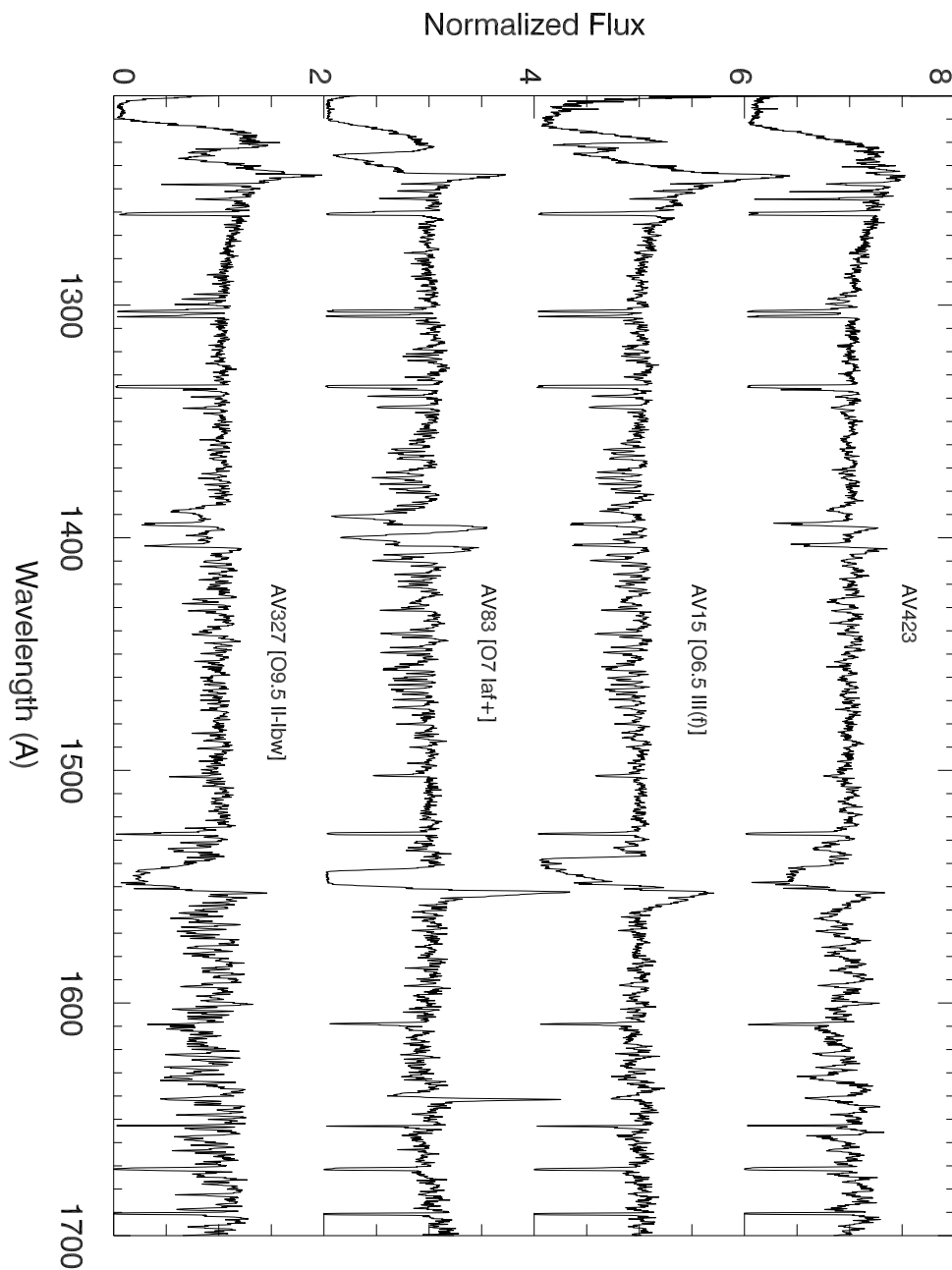


Fig. 3.— STIS spectra of AV 423 (*offset by +6.0*), AV 15 (O6.5 II(f); *offset by +4.0*), AV 83 (O7 Iaf+; *offset by +2.0*), and AV 327 (O9.5 II-Ibw). The current spectral classification of O9.5 V for AV 423 is inconsistent with its UV spectrum.

Table 3. Large Magellanic Cloud Targets

Star	Spectral Classification	$\langle V \sin i \rangle$ (km s ⁻¹)	SWP # or STIS data set
HD 269810	O2 III(f*)	173	O6LZ11010
SK -66 172	O2 III(F*)+OB	68	SWP33971
HD 269698	O4 I	157	SWP08011,06967
HD 269676	O4-5 III(f)	125	O63541010
HD 269676	O4-5 III(f)	156	SWP05086,13908,14022
SK -69 212	[O5 III(f)]	210	SWP52709
LH10-3120	[O5.5 V((f*))]	95	O5EZ01010,01020,01030
SK -66 100	[O6 III]	116	SWP33139
HD 270952	O6 Iaf	61	SWP45216
HD 269357	O6 I	97	SWP04314,55231
SK -67 111	[O6 Ia(n)fp]	209	SWP10991,52745
SK -67 51	[O6.5 III]	105	SWP31341
CD -68 264	[O8 V]	139	SWP47851
SK -67 101	[O8 II((f))]	101	O4YN01010,01020
LH58 52a	[O8 II]	110	SWP49323
SK -67 266	[O8 Iaf]	144	SWP20411
LH58 19a	[O9 II]	178	SWP49312
HD 268605	O9.7 Ib	90	SWP06540,51851,52010
HD 269889	O9.7 Ib	72	SWP47601
HD 269896	ON9.7Ia	70	SWP47594,55216
SK -67 106	[B0 III]	135	O4YN03010
SK -67 107	[B0 III]	103	O4YN04010,04020

the fraction of stars having a $V \sin i$ less than a specific upper value that ranges from zero to the maximum $V \sin i$ observed.

Before comparing the MC samples it is helpful to determine if the cdf of Galactic dwarf (IV-V) stars is different from that of Galactic evolved (I-III) stars. We plot in Figure 4 the CDF for both groups of stars based on the sample in P96. We see that the evolved sample has both fewer slow rotators and fewer fast rotators compared to the unevolved sample. The Kolmogorov-Smirnov (K-S) test determines the probability that two samples are drawn from the same parent population. For the Galactic evolved and unevolved stars this probability is only 16%, which suggests that the differences may be significant. Howarth et al. (1997) came to the same conclusion in their study of projected rotational velocities of Galactic O-stars. They suggest that the evolved stars do indeed spin down as they grow in radius (removing the fastest rotators from the sample) and that there exists excess turbulent broadening among the supergiants (that removes the most narrow-lined stars from the sample).

The differences in the distributions of projected rotational velocity between the unevolved and evolved groups appears to support theoretical models that predict a spin-down during the core H-burning phases of evolution (Heger & Langer 2000; Meynet & Maeder 2000). It is important to recognize that most stars with an O spectral type are probably found in the core H-burning phase, even among the more luminous stars (see the evolutionary tracks of Schaller et al. 1992). Thus, we expect that the low Z , Magellanic Cloud O-stars are also in this phase where the rotational spin-down is predicted to be much less effective than we find in Galactic stars (Maeder & Meynet 2001). The low Z stars should retain an almost constant V_{rot} during their core H-burning evolution. Therefore, we expected that the cumulative distribution function for the low Z stars would fall well below that of Galactic stars, because of the relative excess of rapid rotators.

The existence of a systematic difference between the velocity distributions of Galactic unevolved and evolved O-stars (Fig. 4) indicates that we must compare like samples between the Galactic and Magellanic Cloud stars in order to avoid spurious results because of differing proportions of unevolved and evolved stars in the groups. A large percentage of our Magellanic Cloud samples are objects with evolved luminosity classes (68% and 90% for the SMC and LMC samples, respectively). Note that we include the two SMC stars lacking a luminosity class, AV 80 and AV 220, among the evolved stars since Walborn et al. (2000) find them to have luminosities consistent with an advanced evolutionary state. We also include SMC star AV 423 among the evolved group because of the features in the UV spectrum indicating a high luminosity (see §3). We show in Figure 5 the cumulative distribution functions for the evolved O-stars in the Galaxy, SMC, and LMC. Surprisingly, the distributions for all three samples are very similar, with K-S probabilities of 44% and

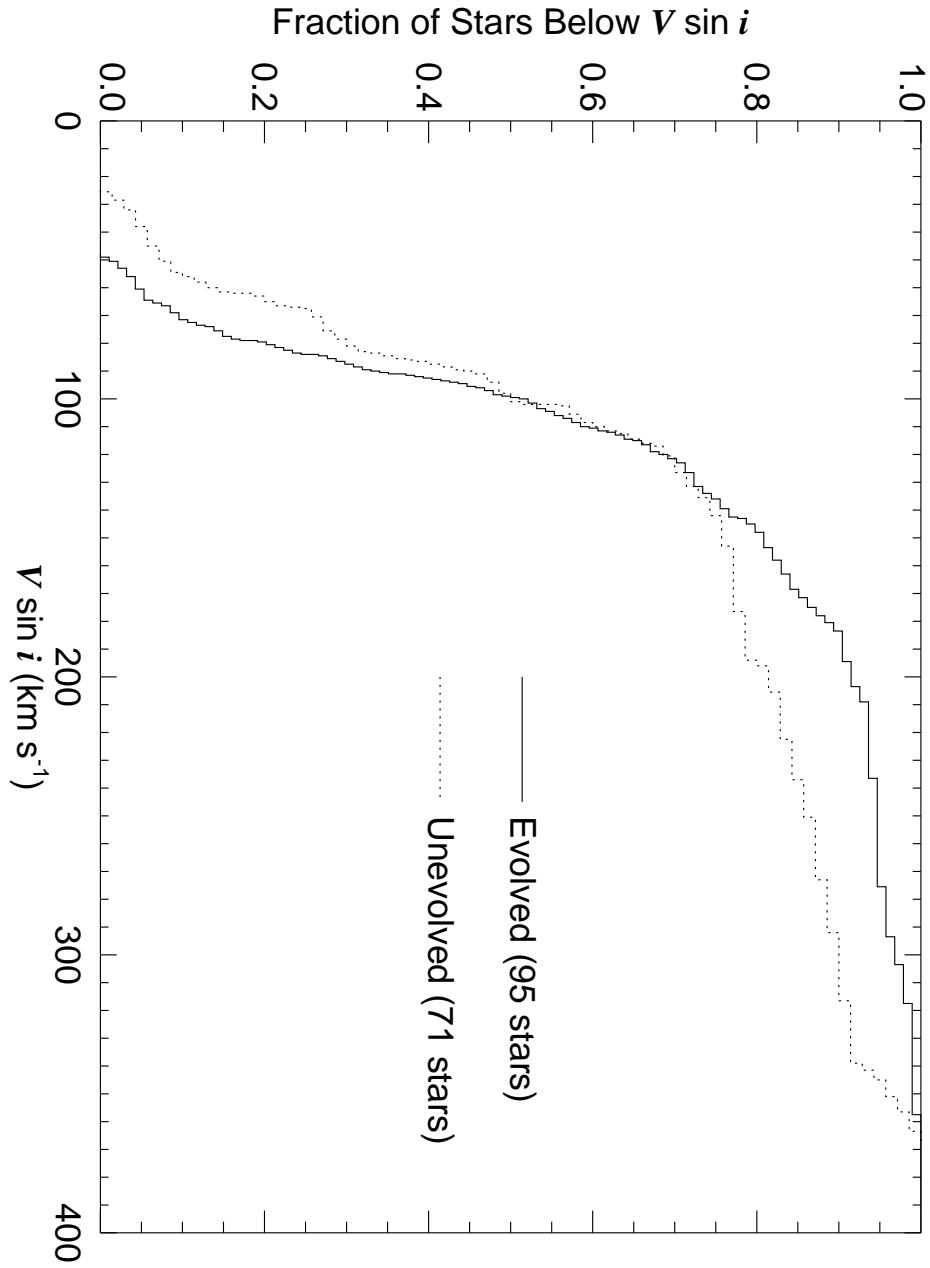


Fig. 4.— The cumulative distributions of projected rotational velocities for Galactic stars from Penny (1996). The dotted line represent those objects with luminosity classes IV and V, while the solid line corresponds to stars with luminosity classes I, II, and III.

42% that the LMC and SMC samples, respectively, are drawn from the same parent population as the Galactic sample. There is no visible trend of cumulative distribution functions with metallicity. The LMC sample has slightly faster $V \sin i$ values than that of the Galactic stars, but the SMC objects have slightly slower rotation rates than the other two samples. There are too few unevolved stars to make a reliable comparison, but the average projected rotational velocities in each group appear to be comparable: $\langle V \sin i \rangle = 131 \pm 93$, 117 ± 31 , and $78 \pm 45 \text{ km s}^{-1}$ for the Galactic, LMC, and SMC unevolved stars, respectively.

Taken at face value, our results do not support the prediction that the low Z stars of the Magellanic Clouds are rapid rotators. However, because of our relatively small sample sizes, we clearly need additional measurements to confirm the the result. Are low Z stars actually rotating at the same speeds as their Galactic counterparts? In order to determine conclusively the answer, a larger number of $V \sin i$ values for stars in these environments is needed. A previous study by Keller (2001) examined the rotation rates of 100 early B-type stars in the LMC. Compared with a similar sample of Galactic stars, the low metallicity stars show larger rotation rates. The largest initial mass of these early B-type stars is only $12 M_{\odot}$ and as such their MS evolution is not expected to be influenced by mass loss. However this is exactly the sort of large scale project which is necessary for the more massive O-type stars. A project with the FLAMES multi-object spectrograph on the VLT to obtain such spectra is currently ongoing. Additionally efforts are underway which focus on observing evolved (I-III classes) early type (O3-O5) stars in the LMC. As these stars should correspond to a later stage in the core H-burning evolution of the most massive stars, they represent a critical test of the current treatment of mass and angular momentum loss in low metallicity massive stars.

Support for this project AR#09945 was provided in part by by NASA through a grant from the Space Telescope Science Institute, which is operated by the Association of Universities for Research in Astronomy, Inc. under NASA contract NAS5-26555. The data presented in this paper were obtained from the Multimission Archive at the Space Telescope Science Institute (MAST). Support for MAST for non-HST data is provided by the NASA Office of Space Science via grant NAG5-7584 and by other grants and contracts.

REFERENCES

- Auer, L. H., & Mihalas, D. 1972, ApJS, 24, 193
 Conti, P. S., & Ebbets, D. 1977, ApJ, 213, 438
 Conti, P. S., Garmany, C. D., & Massey, P. 1986, AJ, 92, 48

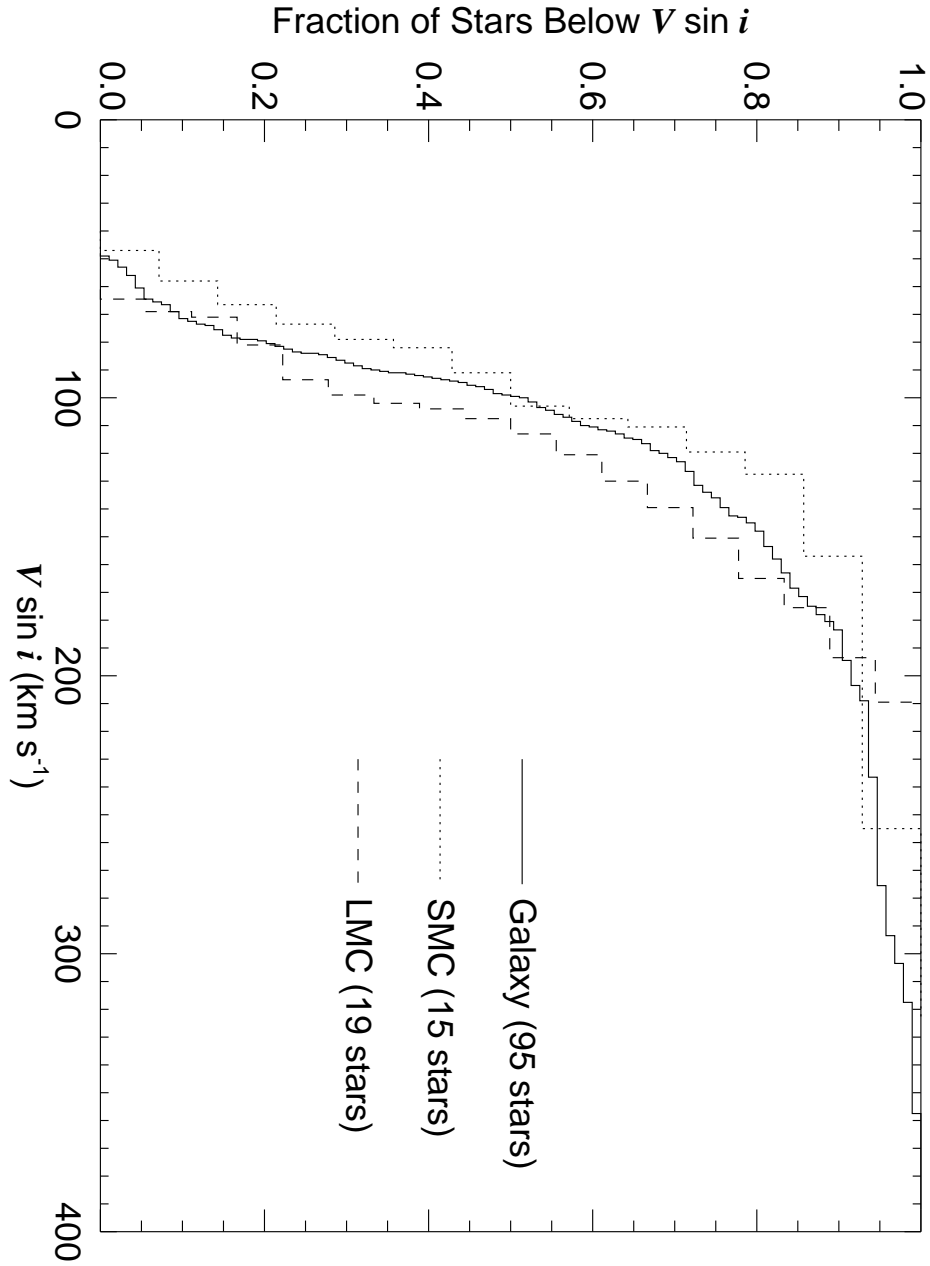


Fig. 5.— The cumulative distribution of projected rotational velocities for 15 SMC (*dotted line*), 19 LMC (*dashed line*), and 95 Galactic (*solid line*) O-type stars of luminosity class I to III.

- Garmany, C. D., Conti, P. S., & Massey, P. 1987, *AJ*, 93, 1070
- Garmany, C. D., Massey, P., & Parker, J. W. 1994, *AJ*, 108, 1256
- Heger, A., & Langer, N. 2000, *ApJ*, 544, 1016
- Howarth, I. D., & Prinja, R. K. 1989, *ApJS*, 69, 527
- Howarth, I. D., Seibert, K. W., Hussain, A. J., & Prinja, R. K. 1997, *MNRAS*, 284, 265
- Howarth, I. D., & Smith, K. C. 2001, *MNRAS*, 327, 353
- Humphreys, R. M., & McElroy, D. B. 1984, *ApJ*, 284, 565
- Keller, S.C. 2001, *PASP*, 113, 1570
- Keller, S. C., Wood, P. R., & Bessell, M. S. 1999, *A&AS*, 134, 489
- Koen, C., & Eyer, L. 2002, *MNRAS*, 331, 45
- MacFadyen, A. I., & Woosley, S. E. 1999, *ApJ*, 524, 262
- Maeder, A., Grebel, E. K., & Mermilliod, J.-C. 1999, *A&A*, 346, 459
- Maeder, A., & Meynet, G. 2001, *A&A*, 373, 555
- Maíz-Apellániz, J., Walborn, N. R., Galué, H. Á., & Wei, L. H. 2004, *ApJS*, 151, 103
- Massey, P., Lang, C. C., Degioia-Eastwood, K., & Garmany, C. D. 1995, *ApJ*, 438, 188
- Massey, P., Parker, J. W., & Garmany, C. D. 1989, *AJ*, 98, 1305
- Massey, P., Silkey, M., Garmany, C. D., & Degioia-Eastwood, K. 1989, *AJ*, 97, 107
- Meynet, G., & Maeder, A. 2000, *A&A*, 346, 459
- Parker, J. W., Garmany, C. D., Massey, P., & Walborn, N. 1992, *AJ*, 103, 1205
- Penny, L. R. 1996, *ApJ*, 463, 737 (P96)
- Penny, L. R. 1997, *PASP*, 109, 848
- Penny, L. R., Gies, D. R., & Bagnuolo, W. G., Jr. 1997, *ApJ*, 483, 439
- Penny, L. R., Seyle, D., Gies, D. R., Harvin, J. A., Bagnuolo, W. G., Jr., Thaller, M. L., Fullerton, A. W., & Kaper, L. 2001, *ApJ*, 548, 889
- Porter, J. M., & Rivinius, T. 2003, *PASP*, 115, 1153
- Schaller, G., Schaerer, D., Meynet, G., & Maeder, A. 1992, *A&AS*, 96, 269
- Venn, K. A., McCarthy, J. K., Lennon, D. J., & Kudritzki, R. P. 1998, in *Boulder-Munich II: Properties of Hot, Luminous Stars*, ed. I. Howarth (San Francisco: ASP), 177

Walborn, N. R., Lennon, D. J., Heap, S. R., Lindler, D. J., Smith, L. J., Evans, C. J., & Parker, J. W. 2000, PASP, 112, 1243 (W00)